

Experimental Observation of Left-Handed Behavior in an Array of Standard Dielectric Resonators

Liang Peng,¹ Lixin Ran,^{1,2,*} Hongsheng Chen,¹ Haifei Zhang,¹ Jin Au Kong,^{1,3} and Tomasz M. Grzegorzczak³

¹Electromagnetics Academy at Zhejiang University, Zhejiang University, Hangzhou 310027, China

²Department of Information and Electronic Engineering, Zhejiang University, Hangzhou 310027, China

³Research Laboratory of Electronics, Massachusetts Institute of Technology, Cambridge, Massachusetts 02139, USA

(Received 7 November 2006; published 12 April 2007)

We demonstrate that by utilizing displacement currents in simple dielectric resonators instead of conduction currents in metallic split-ring resonators and by additionally exciting the proper modes, left-handed properties can be observed in an array of high dielectric resonators. Theoretical analysis and experimental measurements show that the modes, as well as the subwavelength resonance, play an important role in the origin of the left-handed properties. The proposed implementation of a left-handed metamaterial, based on a purely dielectric configuration, opens the possibility of realizing media at terahertz frequencies since scaling issues and losses, two major drawbacks of metal-based structures, are avoided.

DOI: 10.1103/PhysRevLett.98.157403

PACS numbers: 78.20.Ci, 41.20.Jb, 42.25.Fx, 73.20.Mf

The concept of left-handed material (LHM) is now well accepted by both the scientific and the engineering communities. Possessing simultaneously a negative effective permittivity and permeability, LHMs exhibit unique electromagnetic (EM) properties compared with normal, right-handed materials while still obeying Maxwell equations and not violating known physical laws [1,2]. Since the first realization and verification of an artificial LHM at microwave frequencies in 2000 [3], there have been numerous studies on various aspects of LHM, seeking their inner physics and pursuing possible applications. In [4,5], the basic principles inducing an effective negative permittivity in an array of thin metallic wires and an effective negative permeability in an array of split-ring resonators (SRR) are presented, according to which the negative permittivity and permeability are due to a plasmlike effect of the metallic mesostructures and to the low-frequency magnetic resonance of the SRRs, respectively. Various metal-based LHMs have been proposed, including the widely studied rod-SRR structure, Ω ring, S ring, and some other variations [3,6,7]. From the equivalent circuit model (ECM) analysis of metal-based LHMs [8], it has been realized that independently of the shapes of the LHM unit cells, an important task in the design is to actually obtain a subwavelength resonance, from which the left-handed behavior appears in a frequency band corresponding to both an electric and a magnetic resonance. In this Letter we show that, in addition to subwavelength resonance, the modal distribution of the EM fields plays an important role in generating an effective left-handed behavior as well. By exciting specific modes, we show that the left-handed behavior can be observed in simple dielectric resonators. A theoretical analysis as well as experimental measurements of an array composed of high dielectric constant rods, both periodically and randomly arranged, is presented. The closed form analysis and experimental results

indicate that the scattered fields generated by the inner subwavelength modes indeed produce a left-handed behavior.

We start by considering a standard cylindrical dielectric resonator as depicted in Fig. 1(a) and an incident plane wave propagating along the x axis with its electric field \vec{E}_i polarized along the z axis. As functions of the permittivity, multiple modes can be excited within this resonator. In Figs. 1(b) and 1(c), the second resonant mode (the mode of

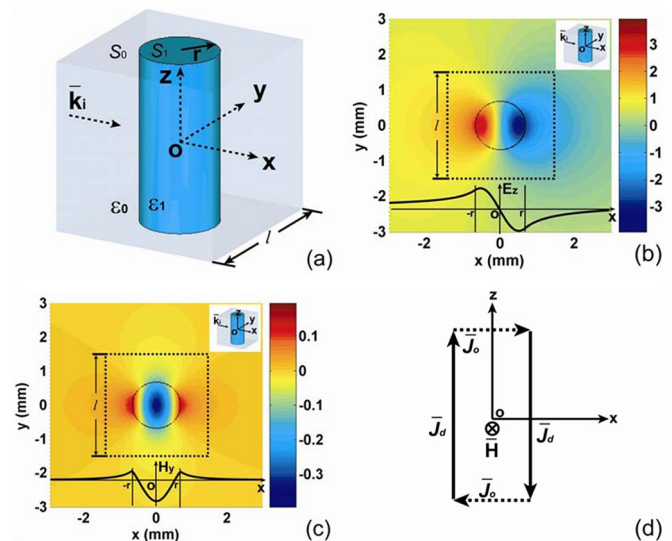


FIG. 1 (color online). Second resonant mode inside a dielectric resonator under a plane wave incidence. (a) Unit cell configuration, (b) electric field distributions, (c) magnetic field distributions, and (d) equivalent current ring. The solid line represents the displacement current \vec{J}_d inside the resonator, and the dashed line represents the outside current \vec{J}_o , which has to be continuous with \vec{J}_d . In the calculation of (b) and (c), $\epsilon_1 = 600$, $r = 0.68$ mm, and the frequency is 6.9 GHz. The incident wave propagates along the x axis and is polarized along the z axis.

interest in this Letter) is calculated by expanding the incident, internal, and scattered fields into vector cylindrical harmonics and imposing the boundary conditions at the surface of the resonator [9]. We see that in such mode the electric field is distributed along the $\pm z$ directions with opposite signs along the propagation direction. When the relative permittivity of the resonator is very high [ε_1 in Fig. 1(a)], an internal subwavelength resonance is set up with a large displacement current ($\varepsilon_1 \varepsilon_0 dE_z/dt$). Realizing that the displacement current plays the same role as the conductive current in Ampère's law, a strong magnetic field H_y is induced by the two contradirectional displacement currents, yielding simultaneously strong electric and magnetic resonances, which can be equivalent to a current ring, as shown in Fig. 1(d). From the displacement current point of view, a dense array of such resonators has a similar topology to the conductive current based rod-SRR array, in which the dense displacement current along the z directions produces a similar plasma behavior as the metallic rod array, and in which the strong magnetic resonance caused by the equivalent current rings acts similarly to the SRRs. Therefore, we expect a similar behavior from the dielectric array structure as from the rod-SRR structure.

In this Letter, we specifically investigate a dielectric resonator array made of a nonmagnetic, ferroelectric ceramic, i.e., $\text{Ba}_{0.5}\text{Sr}_{0.5}\text{TiO}_3$ (BST), which has a relative dielectric constant of about 600 at microwave frequencies and at room temperature without external driving dc voltage [10]. Because of the very high permittivity, the wavelength inside the resonator is "shrunk" by a factor of 24.5, so that more than 10 resonators can be placed in a distance of one wavelength in free space, justifying the use of a homogenization approach [5,11] to calculate the effective constitutive parameters of this dielectric composite. In such a case, the field illuminating each resonator (consisting of the incident field in the absence of the resonators and the field scattered by all the other resonators) can be assumed to be homogeneous inside each unit cell as it has been confirmed by an analytical calculation based on the method presented in [12], which simplifies the calculation without losing accuracy, as shown later.

For simplicity, we assume that the inner fields are uniform along the z direction and therefore we only need to calculate the two-dimensional EM response in the x - y plane inside the unit cell. Following the definition in [11], for periodically arranged unit cells, the effective permittivity along the z direction in each unit cell with a cell constant l is defined by $\varepsilon_{\text{eff},z}(l) = \langle D_{\text{eff},z}(l) \rangle / \langle E_{\text{eff},z}(l) \rangle$, where $\langle D_{\text{eff},z}(l) \rangle$ and $\langle E_{\text{eff},z}(l) \rangle$ denote the averaged electric displacement and electric field strength in each unit cell [5] and

$$\begin{aligned} \langle D_{\text{eff},z}(l) \rangle &= \frac{\varepsilon_0}{l^2} \left[\varepsilon_1 \int_{S_1} \hat{z} \cdot \vec{E}_{\text{int}} dS + \int_{S_0} \hat{z} \cdot (\vec{E}_i + \vec{E}_s) dS \right], \\ \langle E_{\text{eff},z}(l) \rangle &= \frac{1}{S_0} \int_{S_0} \hat{z} \cdot (\vec{E}_i + \vec{E}_s) dS, \end{aligned} \quad (1)$$

where \vec{E}_{int} , \vec{E}_s , and \vec{E}_i represent the internal, the scattered, and the incident electric fields, respectively. $S_1 = \pi r^2$ represents the area of the cross section of the rod and $S_0 = l^2 - S_1$, as shown in Fig. 1. Replacing the integral region S_0 by an annular region S_c whose outer and inner radii are $R = l/\sqrt{\pi}$ and r in Eq. (1), the approximation of $\varepsilon_{\text{eff},z}(l)$ takes the form

$$\varepsilon_{\text{eff},z}(l) \approx \frac{(R^2 - r^2)}{R^2} [1 + I_e(r, R)], \quad (2)$$

where $I_e(r, R) = kr\varepsilon_1 c_0^{(N)} J_1(k_p r) / \{a_0^{(N)} [RH_1^{(1)}(kR) - rH_1^{(1)}(kr)] + RJ_1(kR) - rJ_1(kr)\}$, $k = \omega(\varepsilon_0 \mu_0)^{1/2}$, $k_p = \sqrt{\varepsilon_1} k$, and $a_0^{(N)}$, $c_0^{(N)}$ are corresponding coefficients defined in Ref. [9].

By applying a similar approach, the effective permeability along the y direction can be estimated by

$$\mu_{\text{eff},y}(l) \approx \frac{(R^2 - r^2)}{R^2} [1 - I_h(r, R)], \quad (3)$$

where $I_h(r, R) = i[c_{-1}^{(N)} - c_1^{(N)}]k_p r J_1(k_p r) / \{2[rJ_1(kr) - RJ_1(kR)] + [a_{-1}^{(N)} + a_1^{(N)}][rH_1^{(1)}(kr) - RH_1^{(1)}(kR)]\}$ and $a_m^{(N)}$ and $c_m^{(N)}$ ($m = \pm 1$) are coefficients defined in Ref. [9].

In the case of a random arrangement of resonators, the cell size l is no longer constant. Supposing that l varies within the range $2r < l_{\min} \leq l \leq l_{\max}$, the $\varepsilon_{\text{eff},z}$ and $\mu_{\text{eff},y}$ can be estimated by

$$\varepsilon_{\text{eff},z} \approx \int \varepsilon_{\text{eff},z}(l) f(l) dl, \quad \mu_{\text{eff},y} \approx \int \mu_{\text{eff},y}(l) f(l) dl, \quad (4)$$

where $f(l)$ is the cell fraction function, which can be treated as a probability density distribution function of a unit cell with cell size l . In this Letter, $f(l)$ is assumed to be a uniformly distributed function, or $f(l) = 1/(l_{\max} - l_{\min})$.

Starting from the calculated fields shown in Figs. 1(b) and 1(c) and applying Eqs. (1)–(4), the effective permittivity and permeability of a BST resonator array can be estimated theoretically. Figures 2(a) and 2(b) show the results for a periodically arranged array and a randomly arranged array, respectively. In the calculation, the dielectric constant of the BST is selected to be 600 and the radii of the resonators are all 0.68 mm (in order to be comparable to the later experimental configuration). In the periodic case, the periodicity is 3 mm, while in the randomized case l is distributed between 1.8 and 3.5 mm. We see that in both the periodic and the random cases, the composite exhibits simultaneously a negative permittivity and a negative permeability in a band from 6.89 to 7.23 GHz, showing that the double negative band is dominated by the dimensions of each resonator and has little dependency on their locations (a property drastically different from photonic crystals, for example, where the locations of the dielectric inclusions are fundamentally important). In the frequency range close to resonance, from 3.7 to 5.3 GHz in Fig. 2(b), the integral in Eq. (4) does not converge and we do not expect the effective medium theory to hold.

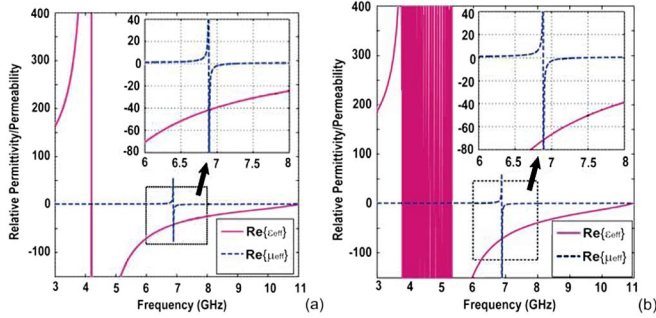


FIG. 2 (color online). Calculation of the effective relative permittivity $\epsilon_{\text{eff},z}$ and the effective relative permeability $\mu_{\text{eff},y}$ of the BST resonator array. (a) Periodic case and (b) random case. The black arrows point to the insets showing the enlarged regions enclosed by the dashed lines.

In the experiment, a bulk BST ceramic manufactured by hot-press technique is cut into 10 mm long rods with square cross sections of 1 mm \times 1 mm, as shown in Fig. 3(a). Note that for technological reasons, square cross sections are used instead of circular ones, without influencing the qualitative results. Two prisms are fabricated by inserting the BST rods into a low-loss foam background: in the first prism, the positions of the rods are periodic while they are random in the second prism, as shown in the insets of Figs. 3(b) and 3(c). The cell constant l is 3 mm for the first prism and is distributed between about 1.5 and about 4 mm for the second. The corresponding angles formed by the long right-angle side and the hypotenuse are 18.4° and 22° , respectively. The experiment is performed in a setup very similar to that in Ref. [13], in which the prisms are placed inside a parallel plate waveguide with good contact between the rods and the waveguide's inner walls to ensure the existence of the predicted modes inside the resonators. The contact also helps to generate large conductive currents on the metal boundaries that link the displacement currents inside the resonators in order to form the closed current rings, so that the equivalent model in Fig. 1(d) is unchanged. The experimental results are shown in Figs. 3(b) and 3(c). We see that in both the periodic and the randomized cases, negative refractions are observed around 7 GHz. Two outgoing beams are observed, however: in Fig. 3(b), the two refractive angles are about -20° and -67° at 7.2 GHz, and in Fig. 3(c) the corresponding angles are about -21° and -63° . We subsequently show that the refractions with larger refractive angles are second order refractions due to the severe mismatch between the prisms and the air. For the first order refractions, the refractive indices calculated from Figs. 3(b) and 3(c) at 7.2 GHz are about -1.08 and -0.96 , respectively. From the theoretical results of Fig. 2, we see that the effective relative permeability is much smaller than the relative permittivity in most of the double negative band, yielding an impedance of the effective medium smaller than that of the air. For an incident electric field \vec{E}_i polarized along the z axis, the symmetry of the structure makes the composite

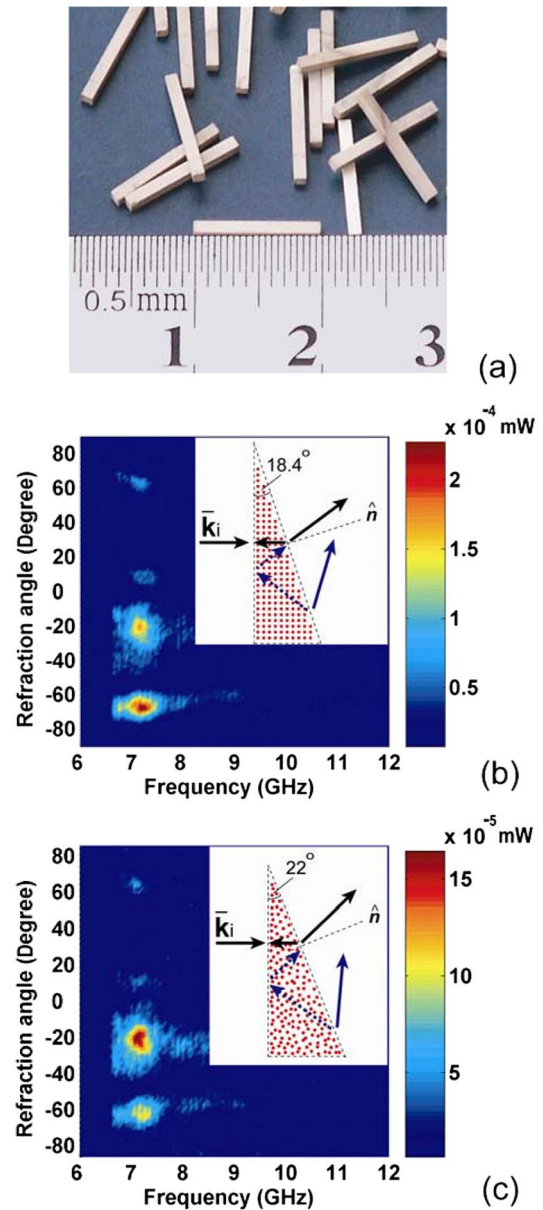


FIG. 3 (color online). Experimental verification of negative refraction. (a) Picture of the BST rods utilized in the experiment, (b) experimental results for a periodically arranged prism, and (c) experimental results for a randomly arranged prism. The notation \hat{n} in (b) and (c) refers to the normal of interface between the prisms and air.

isotropic in the x - y plane, so that we can calculate the second order refractions by a direct application of Snell's law and the above calculated refractive indices, which are shown by dark gray (blue) arrows in Figs. 3(b) and 3(c). The calculated results of -63° and -61° , respectively, are close to the experimental results. We can also notice that in both the periodic and the randomized cases, negative refractions occur in a similar manner, indicating that the negative refraction does not result from the periodicity.

Finally, we show in Fig. 4 the simulated magnetic field distributions for four metal-based unit cells (SRR, Ω ring,

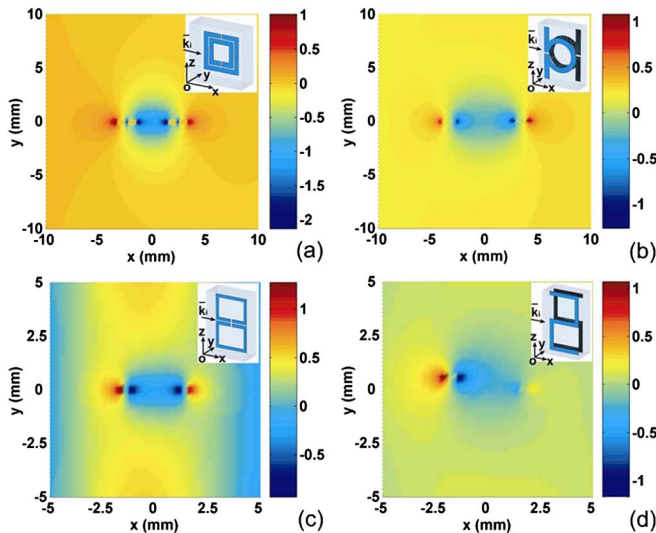


FIG. 4 (color online). Magnetic modes in different metallic resonators at frequencies corresponding to a negative permeability. (a) SRR, (b) Ω ring, (c) symmetrical SRR, and (d) S ring. In all cases, the y components of the magnetic fields in the x - y plane are shown, and have been normalized by the incident magnetic field.

symmetrical SRR, and S ring). Although the shapes of these rings are quite different, the overall distributions of the magnetic fields inside the resonators along the y direction are all similar to that in Fig. 1(c), and the negative permeability vanishes when this mode disappears. From Fig. 4, we conclude that the SRR and its variations can be somewhat equivalent to a simple dielectric resonator composed of a high permittivity and with the corresponding mode. Similar results from earlier works on LHM can be pointed out. In [14], similar EM modes in dielectric resonators have been discussed in negative refraction, where the coupling between resonators has been identified as the major effect producing the negative refraction, while [15] studied the resonance of rods with negative permittivity from a modal point of view. In [16], similar current distribution in the “plasmon mode” in nanowire composite and related negative refraction behavior in optical range have been discussed. In [17], a gold nanostructure exhibiting negative refraction in optical range is presented, in which the magnetic mode is very similar to our case.

In summary, we have demonstrated by a homogenization approach and an experimental verification that, by utilizing the displacement current of the proper mode instead of the classical conductive current, both periodically and randomly arranged arrays consisting of standard dielectric resonators made of high permittivity dielectric can exhibit a left-handed behavior. Simulations of metal-based SRR unit cells further show that, although different SRRs have different geometries yielding different ECM, they all have a magnetic resonance mode similar to the one in the above dielectric resonator. The dense arrangement of resonators allows us to regard such composite as an effective medium with simultaneously negative permittivity and

permeability. These results imply that left-handed behavior is induced by the proper modes as well as by the subwavelength resonances. Apart from the dense periodicity, the fact that the randomized positions do not influence significantly the left-handed properties indicates that such composite is different from some other structures, such as photonic crystals, in which the negative refraction is deeply related to the periodicity and to the cutting method. From an application point of view, the pure-dielectric structure presented in this Letter opens the way to realize left-handed metamaterials at very high frequencies since it avoids scaling and losses issues, two important drawbacks of metal-based structures. In addition, dielectrics with very high permittivities exist in the terahertz band, for example, the SrTiO_3 , whose dielectric constant is still more than 200 at 10 THz [18].

We thank Dr. Kevin Yingyin Zou with Boston Applied Technologies, Inc. for supplying bulk BST sample, and we are grateful for the helpful discussions with Dr. Bae-Ian Wu, Dr. Jiangtao Haungfu, and Dr. Zu-han Gu. This work was supported by the National Natural Science Foundation of China (NSFC) under Grants No. 60531020 and No. 60671003, and in part by ZJNSF under Grant No. R105253.

*Corresponding author.

Electronic address: ranlx@zju.edu.cn

- [1] V. G. Veselago, *Sov. Phys. Usp.* **10**, 509 (1968).
- [2] J. Pacheco *et al.*, *Phys. Rev. Lett.* **89**, 257401 (2002).
- [3] D. R. Smith *et al.*, *Phys. Rev. Lett.* **84**, 4184 (2000).
- [4] J. B. Pendry *et al.*, *Phys. Rev. Lett.* **76**, 4773 (1996).
- [5] J. B. Pendry *et al.*, *IEEE Trans. Microwave Theory Tech.* **47**, 2075 (1999).
- [6] J. T. Huangfu *et al.*, *Appl. Phys. Lett.* **84**, 1537 (2004).
- [7] H. S. Chen *et al.*, *Phys. Rev. E* **70**, 057605 (2004).
- [8] H. S. Chen *et al.*, *Prog. Electromagn. Res. pier* **51**, 231 (2005).
- [9] L. Tsang, J. A. Kong, and K. H. Ding, *Scattering of Electromagnetic Wave* (Wiley, New York, 2000), Vol. 1, p. 41.
- [10] M. Ouaddari *et al.*, *IEEE Trans. Microwave Theory Tech.* **53**, 1390 (2005).
- [11] A. Sihvola, *Electromagnetic Mixing Formulas and Applications* (IEE, London, 1999), p. 41.
- [12] T. M. Grzegorzcyk *et al.*, *Phys. Rev. Lett.* **96**, 113903 (2006).
- [13] R. A. Shelby, D. R. Smith, and S. Schultz, *Science* **292**, 77 (2001).
- [14] E. A. Semouchkina *et al.*, *IEEE Trans. Microwave Theory Tech.* **53**, 1477 (2005).
- [15] G. Shvets and Y. A. Urzhumov, *Phys. Rev. Lett.* **93**, 243902 (2004).
- [16] V. A. Podolskiy *et al.*, *Opt. Express* **11**, 735 (2003).
- [17] R. Sambles, *Nature (London)* **438**, 295 (2005).
- [18] W. L. Wolfe, *Handbook of Military Infrared Technology* (USGPO, Washington, DC, 1965), p. 329.